

*Communications in
Applied
Mathematics and
Computational
Science*

**A HIGHER-ORDER GODUNOV METHOD FOR
RADIATION HYDRODYNAMICS: RADIATION
SUBSYSTEM**

MICHAEL DAVID SEKORA AND JAMES M. STONE

vol. 4 no. 1 2009

A HIGHER-ORDER GODUNOV METHOD FOR RADIATION HYDRODYNAMICS: RADIATION SUBSYSTEM

MICHAEL DAVID SEKORA AND JAMES M. STONE

A higher-order Godunov method for the radiation subsystem of radiation hydrodynamics is presented. A key ingredient of the method is the direct coupling of stiff source term effects to the hyperbolic structure of the system of conservation laws; it is composed of a predictor step that is based on Duhamel's principle and a corrector step that is based on Picard iteration. The method is second-order accurate in both time and space, unsplit, asymptotically preserving, and uniformly well behaved from the photon free streaming (hyperbolic) limit through the weak equilibrium diffusion (parabolic) limit and to the strong equilibrium diffusion (hyperbolic) limit. Numerical tests demonstrate second-order convergence across various parameter regimes.

1. Introduction

Radiation hydrodynamics is a fluid description of matter (plasma) that absorbs and emits electromagnetic radiation and in so doing modifies dynamical behavior. The coupling between matter and radiation is significant in many phenomena related to astrophysics and plasma physics, where radiation comprises a major fraction of the internal energy and momentum and provides the dominant transport mechanism. Radiation hydrodynamics governs the physics of radiation-driven outflows, supernovae, accretion disks, and inertial confinement fusion [Castor 2004; Mihalas and Mihalas 1984]. Such physics is described mathematically by a nonlinear system of conservation laws that is obtained by taking moments of the Boltzmann and photon transport equations. A key difficulty is choosing the frame of reference in which to take the moments of the photon transport equation. In the comoving and mixed frame approaches, one captures the matter/radiation coupling by adding relativistic source terms correct to $\mathcal{O}(u/c)$ to the right side of the conservation laws, where u is the material flow speed and c is the speed of light. These source terms are stiff because of the variation in time/length scales associated with such problems [Mihalas and Klein 1982]. This stiffness causes

MSC2000: 35B40, 35L65, 35M10, 76M12.

Keywords: Godunov methods, radiation hydrodynamics, asymptotic preserving methods, hyperbolic conservation laws, stiff source terms, stiff relaxation.

numerical difficulties and makes conventional methods such as operator splitting and method of lines break down [LeVeque 1992; 2002].

Previous research in numerically solving radiation hydrodynamical problems was carried out by Caster [1972], Pomraning [1973], Mihalas and Klein [1982], and Mihalas and Mihalas [1984]. There are a variety of algorithms for radiation hydrodynamics. One of the simplest approaches was developed by Stone et al. [1992] and implemented in the ZEUS code, which was based on operator splitting and Crank–Nicholson finite differencing. Since then, higher-order Godunov methods have emerged as a valuable technique for solving hyperbolic conservation laws (for example, hydrodynamics), particularly when shock capturing and adaptive mesh refinement is important [Stone et al. 2008]. However, developing upwind differencing methods for radiation hydrodynamics is a difficult mathematical and computational task. In many cases, Godunov methods for radiation hydrodynamics either:

- (i) neglect the heterogeneity of weak/strong coupling and solve the system of equations in an extreme limit [Dai and Woodward 1998; 2000];
- (ii) are based on a manufactured limit and solve a new system of equations that attempts to model the full system [Jin and Levermore 1996; Buet and Despres 2006]; or
- (iii) use a variation on flux limited diffusion [Levermore and Pomraning 1981; Gonzalez et al. 2007].

All of these approaches fail to treat the full generality of the problem. For example, Balsara [1999] proposed a Riemann solver for the full system of equations. However, as pointed out by Lowrie and Morel [2001], Balsara’s method failed to maintain coupling between radiation and matter. Moreover, Lowrie and Morel were critical of the likelihood of developing a Godunov method for full radiation hydrodynamics.

In radiation hydrodynamics, there are three important dynamical scales and each scale is associated with either the material flow (speed of sound), radiation flow (speed of light), or source terms. When the matter-radiation coupling is strong, the source terms define the fastest scale. However, when the matter-radiation coupling is weak, the source terms define the slowest scale. Given such variation, one aims for a scheme that treats the stiff source terms implicitly. Following [Miniati and Colella 2007], this paper presents a method that is a higher-order modified Godunov scheme that directly couples stiff source term effects to the hyperbolic structure of the system of conservation laws; it is composed of a predictor step that is based on Duhamel’s principle and a corrector step that is based on Picard iteration. The method is explicit on the fastest hyperbolic scale (radiation flow) but is unsplit and

fully couples matter and radiation with no approximation made to the full system of equations for radiation hydrodynamics.

A challenge for the modified Godunov method is its use of explicit time differencing when there is a large range in the time scales associated with the problem, $c/a_\infty \gg 1$, where a_∞ is the reference material sound speed. One could have built a fully implicit method that advanced time according to the material flow scale, but a fully implicit approach was not pursued because such methods often have difficulties associated with conditioning, are expensive because of matrix manipulation and inversion, and are usually built into central difference schemes rather than higher-order Godunov methods. An explicit method may even outperform an implicit method if one considers applications that have flows where $c/a_\infty \lesssim 10$. A modified Godunov method that is explicit on the fastest hyperbolic scale (radiation flow) as well as a hybrid method that incorporates a backward Euler upwinding scheme for the radiation components and the modified Godunov scheme for the material components are under construction for full radiation hydrodynamics. A goal of future research is to directly compare these two methods in various limits for different values of c/a_∞ .

2. Radiation hydrodynamics

The full system of equations for radiation hydrodynamics in the Eulerian frame that is correct to $\mathcal{O}(1/\mathbb{C})$ is

$$\frac{\partial \rho}{\partial t} + \nabla \cdot (\mathbf{m}) = 0, \quad (1)$$

$$\frac{\partial \mathbf{m}}{\partial t} + \nabla \cdot \left(\frac{\mathbf{m} \otimes \mathbf{m}}{\rho} \right) + \nabla p = -\mathbb{P} \left[-\sigma_t \left(\mathbf{F}_r - \frac{\mathbf{u} E_r + \mathbf{u} \cdot \mathbf{P}_r}{\mathbb{C}} \right) + \sigma_a \frac{\mathbf{u}}{\mathbb{C}} (T^4 - E_r) \right], \quad (2)$$

$$\frac{\partial E}{\partial t} + \nabla \cdot \left((E + p) \frac{\mathbf{m}}{\rho} \right) = -\mathbb{P} \mathbb{C} \left[\sigma_a (T^4 - E_r) + (\sigma_a - \sigma_s) \frac{\mathbf{u}}{\mathbb{C}} \cdot \left(\mathbf{F}_r - \frac{\mathbf{u} E_r + \mathbf{u} \cdot \mathbf{P}_r}{\mathbb{C}} \right) \right], \quad (3)$$

$$\frac{\partial E_r}{\partial t} + \mathbb{C} \nabla \cdot \mathbf{F}_r = \mathbb{C} \left[\sigma_a (T^4 - E_r) + (\sigma_a - \sigma_s) \frac{\mathbf{u}}{\mathbb{C}} \cdot \left(\mathbf{F}_r - \frac{\mathbf{u} E_r + \mathbf{u} \cdot \mathbf{P}_r}{\mathbb{C}} \right) \right], \quad (4)$$

$$\frac{\partial \mathbf{F}_r}{\partial t} + \mathbb{C} \nabla \cdot \mathbf{P}_r = \mathbb{C} \left[-\sigma_t \left(\mathbf{F}_r - \frac{\mathbf{u} E_r + \mathbf{u} \cdot \mathbf{P}_r}{\mathbb{C}} \right) + \sigma_a \frac{\mathbf{u}}{\mathbb{C}} (T^4 - E_r) \right], \quad (5)$$

$$\mathbf{P}_r = f E_r \text{ (closure relation)}. \quad (6)$$

For the material quantities, ρ is density, \mathbf{m} is momentum, p is pressure, E is total energy density, and T is temperature. For the radiative quantities, E_r is energy density, \mathbf{F}_r is flux, \mathbf{P}_r is pressure, and f is the variable tensor Eddington factor.

In the source terms, σ_a is the absorption cross section, σ_s is the scattering cross section, and $\sigma_t = \sigma_a + \sigma_s$ is the total cross section.

Following [Lowrie et al. 1999; Lowrie and Morel 2001], the system of equations above has been nondimensionalized with respect to the material flow scale so that one can compare hydrodynamical and radiative effects as well as identify terms that are $\mathcal{O}(u/c)$. This scaling gives two important parameters:

$$\mathbb{C} = c/a_\infty, \quad \mathbb{P} = \frac{a_r T_\infty^4}{\rho_\infty a_\infty^2}.$$

\mathbb{C} measures relativistic effects, while \mathbb{P} measures how radiation affects material dynamics and is proportional to the equilibrium radiation pressure over material pressure. $a_r = (8\pi^5 k^4)/(15c^3 h^3)$ is a radiation constant, T_∞ is the reference material temperature, and ρ_∞ is the reference material density.

For this system of equations, one has assumed that scattering is isotropic and coherent in the comoving frame, emission is defined by local thermodynamic equilibrium (LTE), and that spectral averages for the cross-sections can be employed (gray approximation). The coupling source terms are given by the modified Mihalas–Klein description [Lowrie et al. 1999; Lowrie and Morel 2001], which is more general and more accurate than the original Mihalas–Klein [1982] source terms because it maintains an important $\mathcal{O}(1/\mathbb{C}^2)$ term that ensures the correct equilibrium state and relaxation rate to equilibrium.

Before investigating full radiation hydrodynamics, it is useful to examine the radiation subsystem, which is a simpler system that minimizes complexity while maintaining the rich hyperbolic-parabolic behavior associated with the stiff source term conservation laws. This simpler system allows one to develop a reliable and robust numerical method. Consider Equations (4) and (5) for radiation hydrodynamics in one spatial dimension not affected by transverse flow. If one only considers radiative effects and holds the material flow stationary such that $u \rightarrow 0$, then the conservative variables, fluxes, and source terms for the radiation subsystem are given by

$$\frac{\partial E_r}{\partial t} + \mathbb{C} \frac{\partial F_r}{\partial x} = \mathbb{C} \sigma_a (T^4 - E_r), \quad \frac{\partial F_r}{\partial t} + \mathbb{C} f \frac{\partial E_r}{\partial x} = -\mathbb{C} \sigma_t F_r. \quad (7)$$

Motivated by the asymptotic analysis of Lowrie et al. [1999] for full radiation hydrodynamics, one investigates the limiting behavior for this simpler system of equations. For nonrelativistic flows $1/\mathbb{C} = \mathcal{O}(\epsilon)$, where $\epsilon \ll 1$. Assume that there is a moderate amount of radiation in the flow such that $\mathbb{P} = \mathcal{O}(1)$. Furthermore, assume that scattering effects are small such that $\sigma_s/\sigma_t = \mathcal{O}(\epsilon)$. Lastly, assume that the optical depth can be represented as $\mathcal{L} = \ell_{\text{mat}}/\lambda_t = \ell_{\text{mat}} \sigma_t$, where λ_t is the

total mean free path of the photos and $\ell_{\text{mat}} = \mathcal{O}(1)$ is the material flow length scale [Lowrie et al. 1999].

Free streaming limit: $\sigma_a, \sigma_t \sim \mathcal{O}(\epsilon)$. In this regime, the right side of (7) is negligible, so that the system is strictly hyperbolic; $f \rightarrow 1$ and the Jacobian of the quasilinear conservation law has eigenvalues $\pm\mathbb{C}$:

$$\frac{\partial E_r}{\partial t} + \mathbb{C} \frac{\partial F_r}{\partial x} = 0, \quad \frac{\partial F_r}{\partial t} + \mathbb{C} \frac{\partial E_r}{\partial x} = 0, \quad (8)$$

Weak equilibrium diffusion limit: $\sigma_a, \sigma_t \sim \mathcal{O}(1)$. One obtains this limit by plugging in $\sigma_a, \sigma_t \sim \mathcal{O}(1)$, matching terms of like order, and combining the resulting equations. From the definition of the equilibrium state, $E_r = T^4$ and $F_r = -(1/\sigma_t)\partial P_r/\partial x$. Therefore, the system is parabolic and resembles a diffusion equation, where $f \rightarrow 1/3$:

$$\frac{\partial E_r}{\partial t} = \frac{\mathbb{C}}{3\sigma_t} \frac{\partial^2 E_r}{\partial x^2}, \quad F_r = -\frac{1}{3\sigma_t} \frac{\partial E_r}{\partial x}. \quad (9)$$

Strong equilibrium diffusion limit: $\sigma_a, \sigma_t \sim \mathcal{O}(1/\epsilon)$. One obtains this limit by plugging in $\sigma_a, \sigma_t \sim \mathcal{O}(1/\epsilon)$ and following the steps outlined for the weak equilibrium diffusion limit. One can consider the system to be hyperbolic, where $f \rightarrow 1/3$ and the Jacobian of the quasilinear conservation law has eigenvalues $\pm\epsilon$:

$$\frac{\partial E_r}{\partial t} = 0, \quad F_r = 0. \quad (10)$$

Lowrie et al. [1999] investigated an additional limit for full radiation hydrodynamics, the isothermal regime. This limit has some dynamical properties in common with the weak equilibrium diffusion limit, but its defining characteristic is that the material temperature $T(x, t)$ is constant. When considering the radiation subsystem, there is little difference between the weak equilibrium diffusion and isothermal limits because the material quantities, including the material temperature T , do not evolve. T enters the radiation subsystem as a parameter rather than a dynamical quantity.

3. Higher-order Godunov method

In one spatial dimension, systems of conservation laws with source terms have the form

$$\frac{\partial U}{\partial t} + \frac{\partial F(U)}{\partial x} = S(U), \quad (11)$$

where $U : \mathbb{R} \times \mathbb{R} \rightarrow \mathbb{R}^n$ is an n -dimensional vector of conserved quantities. For the radiation subsystem,

$$U = \begin{pmatrix} E_r \\ F_r \end{pmatrix}, \quad F(U) = \begin{pmatrix} \mathbb{C}F_r \\ \mathbb{C}fE_r \end{pmatrix}, \quad S(U) = \begin{pmatrix} \mathbb{C}S_E \\ \mathbb{C}S_F \end{pmatrix} = \begin{pmatrix} \mathbb{C}\sigma_a(T^4 - E_r) \\ -\mathbb{C}\sigma_t F_r \end{pmatrix}.$$

The quasilinear form of this system of conservation laws is

$$\frac{\partial U}{\partial t} + A \frac{\partial U}{\partial x} = S(U), \quad A = \frac{\partial F}{\partial U} = \begin{pmatrix} 0 & \mathbb{C} \\ \mathbb{C}f & 0 \end{pmatrix}. \quad (12)$$

A has eigenvalues $\lambda = \pm f^{1/2}\mathbb{C}$ and it also has right eigenvectors R (stored as columns) and left eigenvectors L (stored as rows):

$$R = \begin{pmatrix} 1 & 1 \\ -f^{1/2} & f^{1/2} \end{pmatrix}, \quad L = \begin{pmatrix} \frac{1}{2} & -\frac{1}{2}f^{-1/2} \\ \frac{1}{2} & \frac{1}{2}f^{-1/2} \end{pmatrix}. \quad (13)$$

Godunov's method obtains solutions to systems of conservation laws by using characteristic information within the framework of a conservative method:

$$U_i^{n+1} = U_i^n - \frac{\Delta t}{\Delta x} (F_{i+1/2} - F_{i-1/2}) + \Delta t S(U_i^n). \quad (14)$$

Numerical fluxes $F_{i\pm 1/2}$ are obtained by solving the Riemann problem at the cell interfaces with left/right states to get $U_{i-1/2}^{n\pm 1/2}$ and computing

$$F_{i\pm 1/2} = F(U_{i\pm 1/2}^{n+1/2}),$$

where i represents the location of a cell center, $i \pm 1/2$ represents the location cell faces to the right and left of i , and superscripts represent the time discretization. An HLLC (Harten–Lax–van Leer–Einfeldt) solver, used in this work, or any other approximate Riemann solver may be employed because the Jacobian $\partial F/\partial U$ for the radiation subsystem is a constant valued matrix and by definition a Roe matrix [LeVeque 1992; 2002; Roe 1981]. This property also implies that one does not need to transform the system into primitive variables ($\nabla_U W$). The power of the method presented in this paper is that the spatial reconstruction, eigenanalysis, and cell-centered updating directly plug into conventional Godunov machinery.

3.1. Predictor step. One computes the flux divergence $(\nabla \cdot F)^{n+1/2}$ by using the quasilinear form of the system of conservation laws and the evolution along Lagrangian trajectories:

$$\frac{DU}{Dt} + A^L \frac{\partial U}{\partial x} = S(U), \quad A^L = A - uI, \quad \frac{DU}{Dt} = \frac{\partial U}{\partial t} + \left(u \frac{\partial}{\partial x}\right)U. \quad (15)$$

From the quasilinear form, one derives a system that includes (at least locally in time and state space) the effects of the stiff source terms on the hyperbolic structure.

Following [Miniati and Colella 2007; Trebotich et al. 2005], one applies Duhamel's principle to the system of conservation laws, thus giving

$$\frac{DU^{\text{eff}}}{Dt} = \mathcal{F}_{\dot{S}_n}(\eta) \left(-A^L \frac{\partial U}{\partial x} + S_n \right), \quad (16)$$

where $\mathcal{F}_{\dot{S}_n}$ is a propagation operator that projects the dynamics of the stiff source terms onto the hyperbolic structure and $\dot{S}_n = \nabla_U S|_{U_n}$. The subscript n designates time $t = t_n$. Since one is considering a first-order accurate predictor step in a second-order accurate predictor-corrector method, one chooses $\eta = \Delta t/2$ and the effective conservation law is

$$\frac{DU}{Dt} + \mathcal{F}_{\dot{S}_n}(\Delta t/2) A^L \frac{\partial U}{\partial x} = \mathcal{F}_{\dot{S}_n}(\Delta t/2) S_n$$

which implies

$$\frac{\partial U}{\partial t} + A_{\text{eff}} \frac{\partial U}{\partial x} = \mathcal{F}_{\dot{S}_n}(\Delta t/2) S_n, \quad (17)$$

where $A_{\text{eff}} = \mathcal{F}_{\dot{S}_n}(\Delta t/2) A^L + uI$. In order to compute $\mathcal{F}_{\dot{S}_n}$, one first computes \dot{S}_n . Since \mathbb{C} , σ_a , and σ_t are constant and one assumes that $\partial T/\partial E_r$, $\partial T/\partial F_r = 0$:

$$\dot{S}_n = \begin{pmatrix} -\mathbb{C}\sigma_a & 0 \\ 0 & -\mathbb{C}\sigma_t \end{pmatrix}. \quad (18)$$

$\mathcal{F}_{\dot{S}_n}$ is derived from Duhamel's principle and is given by

$$\mathcal{F}_{\dot{S}_n}(\Delta t/2) = \frac{1}{\Delta t/2} \int_0^{\Delta t/2} e^{\tau \dot{S}_n} d\tau = \begin{pmatrix} \alpha & 0 \\ 0 & \beta \end{pmatrix}, \quad (19)$$

with

$$\alpha = \frac{1 - e^{-\mathbb{C}\sigma_a \Delta t/2}}{\mathbb{C}\sigma_a \Delta t/2}, \quad \beta = \frac{1 - e^{-\mathbb{C}\sigma_t \Delta t/2}}{\mathbb{C}\sigma_t \Delta t/2}. \quad (20)$$

Before applying $\mathcal{F}_{\dot{S}_n}$ to A_L , it is important to understand that moving-mesh methods can be accommodated in nonrelativistic descriptions of radiation hydrodynamics whenever an Eulerian frame treatment is employed. These methods do not require transformation to the comoving frame [Lowrie and Morel 2001]. Since the nondimensionalization is associated with the hydrodynamic scale, one can use $u_{\text{mesh}} = u$ from Lagrangean hydrodynamic methods.

The effects of the stiff source terms on the hyperbolic structure are accounted for by transforming to a moving-mesh (Lagrangean) frame $A_L = A - uI$, applying the propagation operator $\mathcal{F}_{\dot{S}_n}$ to A_L , and transforming back to an Eulerian frame $A_{\text{eff}} = \mathcal{F}_{\dot{S}_n} A_L + uI$ [Miniati and Colella 2007]. However, because only the radiation subsystem of radiation hydrodynamics is considered $u_{\text{mesh}} = u \rightarrow 0$. Therefore, the

effective Jacobian is given by

$$A_{\text{eff}} = \begin{pmatrix} 0 & \alpha\mathbb{C} \\ \beta f\mathbb{C} & 0 \end{pmatrix}, \quad (21)$$

which has eigenvalues $\lambda_{\text{eff}} = \pm(\alpha\beta)^{1/2} f^{1/2}\mathbb{C}$ with the limits

$$\sigma_a, \sigma_t \rightarrow 0 \Rightarrow \alpha, \quad \beta \rightarrow 1 \Rightarrow \lambda_{\text{eff}} \rightarrow \pm f^{1/2}\mathbb{C} \quad (\text{free streaming}), \quad (22)$$

$$\sigma_a, \sigma_t \rightarrow \infty \Rightarrow \alpha, \quad \beta \rightarrow 0 \Rightarrow \lambda_{\text{eff}} \rightarrow \pm\epsilon \quad (\text{strong equilibrium diffusion}).$$

A_{eff} has right eigenvectors R_{eff} (stored as columns) and left eigenvectors L_{eff} (stored as rows):

$$R_{\text{eff}} = \begin{pmatrix} 1 & 1 \\ -(\beta f/\alpha)^{1/2} & (\beta f/\alpha)^{1/2} \end{pmatrix}, \quad L_{\text{eff}} = \begin{pmatrix} \frac{1}{2} & -\frac{1}{2}(\alpha/\beta f)^{1/2} \\ \frac{1}{2} & \frac{1}{2}(\alpha/\beta f)^{1/2} \end{pmatrix}. \quad (23)$$

3.2. Corrector step. The time discretization for the source term is a single-step, second-order accurate scheme based on the ideas from [Dutt et al. 2000; Minion 2003; Miniati and Colella 2007]. Given the system of conservation laws, one aims for a scheme that has an explicit approach for the conservative flux divergence term $\nabla \cdot F$ and an implicit approach for the stiff source term $S(U)$. Therefore, one solves a following collection of ordinary differential equations at each grid point:

$$\frac{dU}{dt} = S(U) - (\nabla \cdot F)^{n+1/2}, \quad (24)$$

where the time-centered flux divergence term is taken to be a constant source which is obtained from the predictor step. Assuming time $t = t_n$, the initial guess for the solution at the next time step is

$$\hat{U} = U^n + \Delta t (I - \Delta t \nabla_U S(U)|_{U^n})^{-1} (S(U^n) - (\nabla \cdot F)^{n+1/2}), \quad (25)$$

where

$$(I - \Delta t \nabla_U S(U)) = \begin{pmatrix} 1 + \Delta t \mathbb{C} \sigma_a & 0 \\ 0 & 1 + \Delta t \mathbb{C} \sigma_t \end{pmatrix}, \quad (26)$$

$$(I - \Delta t \nabla_U S(U))^{-1} = \begin{pmatrix} (1 + \Delta t \mathbb{C} \sigma_a)^{-1} & 0 \\ 0 & (1 + \Delta t \mathbb{C} \sigma_t)^{-1} \end{pmatrix}. \quad (27)$$

The error ϵ is defined as the difference between the initial guess and the solution obtained from the Picard iteration equation, where the initial guess was used as a starting value:

$$\epsilon(\Delta t) = U^n + \frac{\Delta t}{2} (S(\hat{U}) + S(U^n)) - \Delta t (\nabla \cdot F)^{n+1/2} - \hat{U}. \quad (28)$$

Following [Miniati and Colella 2007], the correction to the initial guess is given by

$$\delta(\Delta t) = (I - \Delta t \nabla_U S(U)|_{\hat{U}})^{-1} \epsilon(\Delta t). \quad (29)$$

Therefore, the solution at time $t = t_n + \Delta t$ is

$$U^{n+1} = \hat{U} + \delta(\Delta t). \quad (30)$$

3.3. Stability and algorithmic issues. The higher-order Godunov method satisfies important conditions that are required for numerical stability [Miniati and Colella 2007]. First, $\lambda_{\text{eff}} = \pm(\alpha\beta)^{1/2} f^{1/2} \mathbb{C}$ indicates that the subcharacteristic condition for the characteristic speeds at equilibrium is always satisfied, such that: $\lambda^- < \lambda_{\text{eff}}^- < \lambda^0 < \lambda_{\text{eff}}^+ < \lambda^+$. This condition is necessary for the stability of the system and guarantees that the numerical solution tends to the solution of the equilibrium equation as the relaxation time tends to zero. Second, since the structure of the equations remains consistent with respect to classic Godunov methods, one expects the CFL (Courant–Friedrichs–Lewy) condition to apply: $\max(|\lambda^*|)(\Delta t/\Delta x) \leq 1$, for $* = -, 0, +$.

Depending upon how one carries out the spatial reconstruction to solve the Riemann problem in Godunov’s method, the solution is either first-order accurate in space (piecewise constant reconstruction) or second-order accurate in space (piecewise linear reconstruction). Piecewise linear reconstruction was employed in this paper, where left/right states (with respect to the cell center) are modified to account for the stiff source term effects [Miniati and Colella 2007; Colella 1990]:

$$\begin{aligned} U_{i,\pm}^n &= U_i^n + \frac{\Delta t}{2} \mathcal{J}_{S_n} \left(\frac{\Delta t}{2} \right) S(U_i^n) + \frac{1}{2} \left(\pm I - \frac{\Delta t}{\Delta x} A_{\text{eff}}^n \right) P_{\pm}(\Delta U_i), \\ P_{\pm}(\Delta U_i) &= \sum_{\pm \lambda_k > 0} (L_{\text{eff}}^k \cdot \Delta U_i) \cdot R_{\text{eff}}^k. \end{aligned} \quad (31)$$

Left/right one-sided slopes as well as cell center slopes are defined for each cell centered quantity U_i . A van Leer limiter is applied to these slopes to ensure monotonicity, thus giving the local slope ΔU_i .

4. Numerical tests

Four numerical tests spanning a range of mathematical and physical behavior were carried out to gauge the temporal and spatial accuracy of the higher-order Godunov method. The numerical solution is compared with the analytic solution where possible. Otherwise, a self-similar comparison is made. Using piecewise constant reconstruction for the left/right states, one can show that the Godunov method reduces to a consistent discretization in each of the limiting cases.

The optical depth τ is a useful quantity for classifying the limiting behavior of a system that is driven by radiation hydrodynamics:

$$\tau = \int_{x_{\min}}^{x_{\max}} \sigma_t dx = \sigma_t (x_{\max} - x_{\min}), \quad (32)$$

Optically thin/thick regimes are characterized by

$$\begin{aligned} \tau < O(1) & \quad (\text{optically thin}), \\ \tau > O(1) & \quad (\text{optically thick}). \end{aligned}$$

In optically thin regimes (free streaming limit), radiation and hydrodynamics decouple such that the resulting dynamics resembles an advection process. In optically thick regimes (weak/strong equilibrium diffusion limit), radiation and hydrodynamics are strongly coupled and the resulting dynamics resembles a diffusion process.

We use the following definitions for the norms and convergence rates throughout this paper. Given the numerical solution q^r at resolution r and the analytic solution u , the error at a given point i is: $\epsilon_i^r = q_i^r - u$. Likewise, given the numerical solution q^r at resolution r and the numerical solution q^{r+1} at the next finer resolution $r+1$ (properly spatially averaged onto the coarser grid), the error resulting from this self-similar comparison at a given point i is: $\epsilon_i^r = q_i^r - q_i^{r+1}$. The 1-norm and max-norm of the error are

$$L_1 = \sum_i |\epsilon_i^r| \Delta x^r, \quad L_{\max} = \max_i |\epsilon_i^r|. \quad (33)$$

The convergence rate is measured using Richardson extrapolation:

$$R_n = \frac{\ln(L_n(\epsilon^r)/L_n(\epsilon^{r+1}))}{\ln(\Delta x^r/\Delta x^{r+1})}. \quad (34)$$

4.1. Exponential growth/decay to thermal equilibrium. The first numerical test examines the temporal accuracy of how variables are updated in the corrector step. Given the radiation subsystem and the initial conditions

$$E_r^0 = \text{constant across space}, \quad F_r^0 = 0, \quad T = \text{constant across space},$$

We have $F_r \rightarrow 0$ for all time. Therefore, the radiation subsystem reduces to the ordinary differential equation

$$\frac{dE_r}{dt} = \mathbb{C}\sigma_a(T^4 - E_r), \quad (35)$$

which has the analytic solution

$$E_r = T^4 + (E_r^0 - T^4)\exp(-\mathbb{C}\sigma_a t). \quad (36)$$

For $E_r^0 < T^4$ and $F_r^0 = 0$, one expects exponential growth in E_r until thermal equilibrium ($E_R = T^4$) is reached. For $E_r^0 > T^4$ and $F_r^0 = 0$, one expects exponential decay in E_r until thermal equilibrium is reached. This numerical test allows one to examine the order of accuracy of the stiff ODE integrator.

Parameters:

$$\mathbb{C} = 10^5, \quad \sigma_a = 1, \quad \sigma_t = 2, \quad f = 1,$$

$$N_{\text{cell}} = [32, 64, 128, 256],$$

$$x_{\min} = 0, \quad x_{\max} = 1, \quad \Delta x = \frac{x_{\min} - x_{\max}}{N_{\text{cell}}}, \quad \text{CFL} = 0.5, \quad \Delta t = \frac{\text{CFL} \Delta x}{f^{1/2} \mathbb{C}},$$

$$\text{IC for growth: } E_r^0 = 1, \quad F_r^0 = 0, \quad T = 10,$$

$$\text{IC for decay: } E_r^0 = 10^4, \quad F_r^0 = 0, \quad T = 1.$$

From [Figure 1](#), one sees that the numerical solution corresponds with the analytic solution. In [Table 1](#) on the next page, the errors and convergence rates are seen to be identical for growth and decay. This symmetry illustrates the robustness of the Godunov method. Furthermore, one finds that the method is well behaved and obtains the correct solution with second-order accuracy for stiff values of the e folding time ($\Delta t \sigma_a \mathbb{C} \geq 1$), although with a significantly larger amplitude in the norm of the error. This result credits the flexibility of the temporal integrator in the corrector step.

In a similar test, the initial conditions for the radiation energy and flux are zero and the temperature is defined by some spatially varying profile (a Gaussian pulse). As time increases, the radiation energy grows into $T(x)^4$. Unless the opacity is sufficiently high, the radiation energy approaches but does not equal $T(x)^4$. This

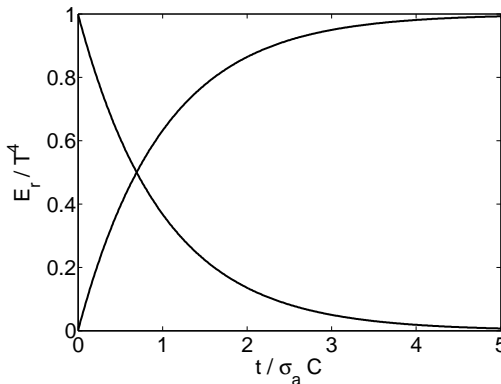


Figure 1. Exponential growth/decay to thermal equilibrium; $N_{\text{cell}} = 256$.

N_{cell}	$L_1(E_r^g)$	Rate	$L_\infty(E_r^g)$	Rate	$L_1(E_r^d)$	Rate	$L_\infty(E_r^d)$	Rate
32	1.4E-1	–	1.4E-1	–	1.4E-1	–	1.4E-1	–
64	3.7E-2	2.0	3.7E-2	2.0	3.7E-2	2.0	3.7E-2	2.0
128	9.3E-3	2.0	9.3E-3	2.0	9.3E-3	2.0	9.3E-3	2.0
256	2.3E-3	2.0	2.3E-3	2.0	2.3E-3	2.0	2.3E-3	2.0

Table 1. Errors and convergence rates for exponential growth and decay in E_r to thermal equilibrium. Errors were obtained through analytic comparison. $t = 10^{-5} = 1/\sigma_a \mathbb{C}$.

result shows that the solution has reached thermal equilibrium and any spatially varying temperature will diffuse.

4.2. Free streaming limit. In the free streaming limit, $\tau \ll O(1)$ and the radiation subsystem reduces to (8). If one takes an additional temporal and spatial partial derivative of the radiation subsystem in the free streaming limit and subtracts the resulting equations, then one finds two decoupled wave equations that have the analytic solutions

$$E_r(x, t) = E_0(x - f^{1/2}\mathbb{C}t), \quad F_r(x, t) = F_0(x - f^{1/2}\mathbb{C}t). \quad (37)$$

Parameters:

$$\mathbb{C} = 10^5, \quad \sigma_a = 10^{-6}, \quad \sigma_t = 10^{-6}, \quad f = 1, \quad T = 1,$$

$$N_{\text{cell}} = [32, 64, 128, 256],$$

$$x_{\min} = 0, \quad x_{\max} = 1, \quad \Delta x = \frac{x_{\min} - x_{\max}}{N_{\text{cell}}}, \quad \text{CFL} = 0.5, \quad \Delta t = \frac{\text{CFL} \Delta x}{f^{1/2}\mathbb{C}},$$

$$\text{IC for Gaussian pulse: } E_r^0, F_r^0 = \exp(-(\nu(x - \mu))^2), \quad \nu = 20, \quad \mu = 0.3,$$

$$\text{IC for square pulse: } E_r^0, F_r^0 = \begin{cases} 1 & \text{if } 0.2 < x < 0.4, \\ 0 & \text{otherwise.} \end{cases}$$

Since the Gaussian pulse results from smooth initial data, one expects $R_1 = 2.0$. However, the square wave results from discontinuous initial data and one expects $R_1 \simeq 0.67$. This is true for all second-order spatially accurate numerical methods when applied to an advection-type problem ($u_t + au_x = 0$) [LeVeque 1992]. See Figure 2 for the shape of the pulses in the free streaming limit, and Table 2 for the corresponding errors and convergence rates.

4.3. Weak equilibrium diffusion limit. In the weak equilibrium diffusion limit, $\tau > O(1)$ and the radiation subsystem reduces to (9). The optical depth suggests the range of total opacities for which diffusion is observed: if $\tau = \sigma_t \ell_{\text{diff}} > 1$,

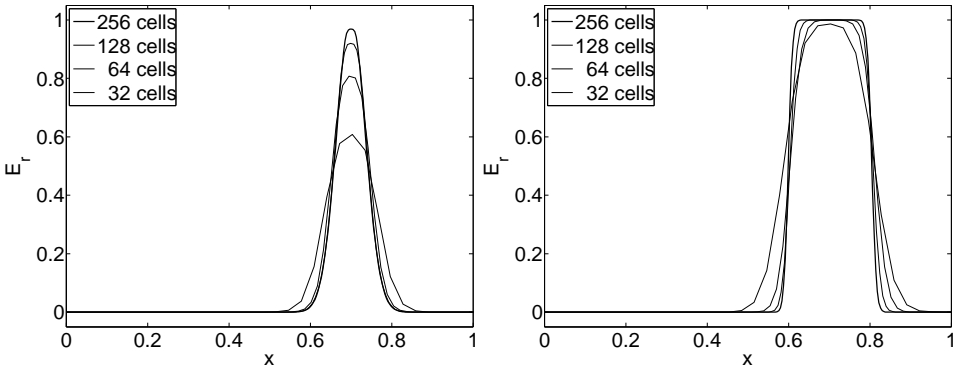


Figure 2. Gaussian pulse (left) and square pulse (right) in free streaming limit; $t = 4 \times 10^{-6} = 0.4(x_{\max} - x_{\min})/C$.

Gaussian pulse

N_{cell}	$L_1(E_r)$	Rate	$L_\infty(E_r)$	Rate	$L_1(F_r)$	Rate	$L_\infty(F_r)$	Rate
32	3.8E-2	–	3.9E-1	–	3.8E-2	–	3.9E-1	–
64	1.3E-2	1.5	1.8E-1	1.1	1.3E-2	1.5	1.8E-1	1.1
128	3.6E-3	1.9	8.0E-2	1.2	3.6E-3	1.9	8.0E-2	1.2
256	8.6E-4	2.1	3.1E-2	1.4	8.6E-4	2.1	3.1E-2	1.4

square pulse

N_{cell}	$L_1(E_r)$	Rate	$L_1(F_r)$	Rate
32	6.0E-2	–	6.0E-2	–
64	4.2E-2	0.5	4.2E-2	0.5
128	2.6E-2	0.7	2.6E-2	0.7
256	1.5E-2	0.8	1.5E-2	0.8

Table 2. Errors (obtained through analytic comparison) and convergence rates for Gaussian and square pulses in free streaming limit; $t = 4 \times 10^{-6} = 0.4(x_{\max} - x_{\min})/C$.

then one expects diffusive behavior for $\sigma_t > 1/\ell_{\text{diff}}$. Additionally, Equation (9) sets the time scale t_{diff} and length scale ℓ_{diff} for diffusion, where $t_{\text{diff}} \sim \ell_{\text{diff}}^2/D$ and $D = fC/\sigma_t$ for the radiation subsystem. Given a diffusion problem for a Gaussian pulse defined over the entire real line ($u_t - Du_{xx} = 0$), the analytic solution is given by the method of Green’s functions:

$$u(x, t) = \int_{-\infty}^{\infty} f(\bar{x})G(x, t; \bar{x}, 0)d\bar{x} = \frac{1}{(4Dt\nu^2 + 1)^{1/2}} \exp\left(\frac{-(\nu(x-\mu))^2}{4Dt\nu^2 + 1}\right). \quad (38)$$

Parameters:

$$\mathbb{C} = 10^5, \quad \sigma_a = 40, \quad \sigma_t = 40, \quad f = 1/3, \quad T^4 = E_r,$$

$$N_{\text{cell}} = [320, 640, 1280, 2560],$$

$$x_{\min} = -5, \quad x_{\max} = 5, \quad \Delta x = \frac{x_{\min} - x_{\max}}{N_{\text{cell}}}, \quad \text{CFL} = 0.5, \quad \Delta t = \frac{\text{CFL} \Delta x}{f^{1/2} \mathbb{C}},$$

$$\text{IC for Gaussian pulse: } \begin{cases} E_r^0 = \exp(-(v(x - \mu))^2), \quad v = 20, \quad \mu = 0.3, \\ F_r^0 = -\frac{f}{\sigma_t} \frac{\partial E_r^0}{\partial x} = \frac{2fv^2(x - \mu)}{\sigma_t} E_r^0 \end{cases}$$

One’s intuition about diffusive processes is based on an infinite domain. So to minimize boundary effects in the numerical calculation, the computational domain and number of grid cells were expanded by a factor of 10. In [Figure 3](#), one observes the diffusive behavior expected for this parameter regime. Additionally, the numerical solution compares well with the analytic solution for a diffusion process defined over the entire real line (38). However, diffusive behavior is only a first-order approximation to more complicated hyperbolic-parabolic dynamics taking place in radiation hydrodynamics as well as the radiation subsystem. Therefore, one needs to compare the numerical solution self-similarly. In [Table 3](#), one sees convergence results for two different time steps: a hyperbolic time step $\Delta t_h = \text{CFL} \Delta x / (f^{1/2} \mathbb{C})$, and parabolic one, $\Delta t_p = \text{CFL} (\Delta x)^2 / (2D)$. This difference in the convergence rate results from the temporal accuracy in the numerical solution. In the weak equilibrium diffusion limit, the Godunov method reduces to a forward-time/centered-space discretization of the diffusion equation. Such a discretization requires a parabolic time step $\Delta t \sim (\Delta x)^2$ in order to see second-order convergence because the truncation error of the forward-time/centered-space discretization of the diffusion equation is $\mathcal{O}(\Delta t, (\Delta x)^2)$.

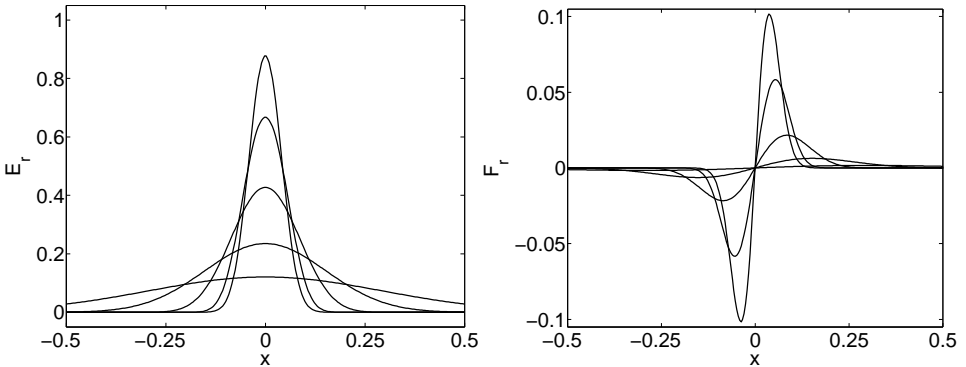


Figure 3. E_r (left) and F_r (right) in weak equilibrium diffusion limit; $t = [0.25, 1, 4, 16, 64] \times 10^{-6}$.

Hyperbolic time step: $\Delta t_h = \text{CFL } \Delta x / (f^{1/2} \mathbb{C})$

N_{cell}	$L_1(E_r)$	Rate	$L_\infty(E_r)$	Rate	$L_1(F_r)$	Rate	$L_\infty(F_r)$	Rate
320	8.9E-3	–	4.5E-2	–	1.1E-3	–	3.7E-3	–
640	6.6E-3	0.4	3.4E-2	0.4	8.3E-4	0.4	3.1E-3	0.2
1280	3.4E-3	1.0	1.6E-2	1.1	4.1E-4	1.0	1.4E-3	1.2
2560	1.6E-3	1.1	7.1E-3	1.1	1.9E-4	1.1	6.0E-4	1.2

Parabolic time step: $\Delta t_p = \text{CFL } (\Delta x)^2 / (2D)$

N_{cell}	$L_1(E_r)$	Rate	$L_\infty(E_r)$	Rate	$L_1(F_r)$	Rate	$L_\infty(F_r)$	Rate
320	1.7E-2	–	8.3E-2	–	2.0E-3	–	7.9E-3	–
640	5.0E-3	1.7	2.5E-2	1.7	6.0E-4	1.7	2.0E-3	2.0
1280	1.1E-3	2.2	5.1E-3	2.3	1.3E-4	2.3	3.6E-4	2.4
2560	2.5E-4	2.1	1.2E-3	2.1	2.8E-5	2.2	7.4E-5	2.3

Table 3. Errors (obtained through analytic comparison) and convergence rates for E_r and F_r in the weak equilibrium diffusion limit, when time is advanced according to each indicated scheme; $t = 4 \times 10^{-6}$.

4.4. Strong equilibrium diffusion limit. In the strong equilibrium diffusion limit, $\tau \gg O(1)$. From (10), we have $F_r \rightarrow 0$ for all time and space while $E_r = E_r^0$.

Parameters:

$$\mathbb{C} = 10^5, \quad \sigma_a = 10^6, \quad \sigma_t = 10^6, \quad f = 1/3, \quad T^4 = E_r,$$

$$N_{\text{cell}} = [320, 640, 1280, 2560],$$

$$x_{\min} = -5, \quad x_{\max} = 5, \quad \Delta x = \frac{x_{\min} - x_{\max}}{N_{\text{cell}}}, \quad \text{CFL} = 0.5, \quad \Delta t = \frac{\text{CFL } \Delta x}{f^{1/2} \mathbb{C}},$$

$$\text{IC for Gaussian Pulse: } \begin{cases} E_r^0 = \exp(-(v(x - \mu))^2), \quad v = 20, \quad \mu = 0.3, \\ F_r^0 = -\frac{f}{\sigma_t} \frac{\partial E_r^0}{\partial x} = \frac{2fv^2(x - \mu)}{\sigma_t} E_r^0 \end{cases}$$

In this test, the numerical solution is held fixed at the initial distribution because σ_a, σ_t are so large. However, if one fixed ℓ_{diff} and scaled time according to

$$t_{\text{diff}} \approx \ell_{\text{diff}}^2 / D = \ell_{\text{diff}}^2 \sigma_t / f \mathbb{C},$$

then one would observe behavior similar to Figure 3. This test illustrates the robustness of the Godunov method to handle very stiff source terms. (See Table 4 for errors and convergence rates.)

N_{cell}	$L_1(E_r)$	Rate	$L_\infty(E_r)$	Rate
320	2.2E-3	–	1.8E-2	–
640	5.3E-4	2.1	5.6E-3	1.6
1280	1.3E-4	2.0	1.5E-3	1.9
2560	3.3E-5	2.0	3.8E-4	2.0

Table 4. Errors and convergence rates for E_r in the strong equilibrium diffusion limit. Errors were obtained through self-similar comparison. $t = 4 \times 10^{-6}$.

5. Conclusions and future work

This paper presents a Godunov method for the radiation subsystem of radiation hydrodynamics that is second-order accurate in both time and space, unsplit, asymptotically preserving, and uniformly well behaved. Moreover, the method employs familiar algorithmic machinery without a significant increase in computational cost. This work is the starting point for developing a Godunov method for full radiation hydrodynamics. The ideas in this paper should easily extend to the full system in one and multiple dimensions using the MUSCL (monotone upstream-centered schemes for conservation laws) or CTU (corner transport upwind) approaches of [Colella 1990]. A modified Godunov method that is explicit on the fastest hyperbolic scale (radiation flow) as well as a hybrid method that incorporates a backward Euler upwinding scheme for the radiation components and the modified Godunov scheme for the material components are under construction for full radiation hydrodynamics. A goal of future research is to directly compare these two methods in various limits for different values of c/a_∞ . Nevertheless, one expects the modified Godunov method that is explicit on the fastest hyperbolic scale to exhibit second-order accuracy for all conservative variables and the hybrid method to exhibit first-order accuracy in the radiation variables and second-order accuracy in the material variables. Work is also being conducted on applying short characteristic and Monte Carlo methods to solve the photon transport equation and obtain the variable tensor Eddington factors. In the present work, these factors were taken to be constant in their respective limits.

Acknowledgment

The authors thank Dr. Phillip Colella for many helpful discussions. MS acknowledges support from the DOE CSGF Program which is provided under grant DE-FG02-97ER25308. JS acknowledges support from grant DE-FG52-06NA26217.

References

- [Balsara 1999] D. S. Balsara, “Linearized formulation of the Riemann problem for radiation hydrodynamics”, *Journal of Quant. Spect. and Radiative Transfer* **61** (1999), 629–635.
- [Buet and Despres 2006] C. Buet and B. Despres, “Asymptotic preserving and positive schemes for radiation hydrodynamics”, *J. Comput. Phys.* **215**:2 (2006), 717–740. [MR 2007j:85005](#) [Zbl 1090.76046](#)
- [Castor 1972] J. I. Castor, “Radiative transfer in spherically symmetric flows”, *Astrophys. Journal* **178** (1972), 779–792.
- [Castor 2004] J. I. Castor, *Radiation Hydrodynamics*, Cambridge University Press, Cambridge, 2004.
- [Colella 1990] P. Colella, “Multidimensional upwind methods for hyperbolic conservation laws”, *J. Comput. Phys.* **87**:1 (1990), 171–200. [MR 91c:76087](#) [Zbl 0694.65041](#)
- [Dai and Woodward 1998] W. Dai and P. R. Woodward, “Numerical simulations for radiation hydrodynamics, I: Diffusion limit”, *J. Comput. Phys.* **142**:1 (1998), 182–207. [MR 99a:76094](#) [Zbl 0933.76057](#)
- [Dai and Woodward 2000] W. W. Dai and P. R. Woodward, “Numerical simulations for radiation hydrodynamics. II. Transport limit”, *J. Comput. Phys.* **157**:1 (2000), 199–233. [MR 2000j:76110](#) [Zbl 0941.76060](#)
- [Dutt et al. 2000] A. Dutt, L. Greengard, and V. Rokhlin, “Spectral deferred correction methods for ordinary differential equations”, *BIT* **40**:2 (2000), 241–266. [MR 2001e:65104](#) [Zbl 0959.65084](#)
- [Gonzalez et al. 2007] M. Gonzalez, E. Audit, and P. Huynh, “HERACLES: a three-dimensional radiation hydrodynamics code”, *Astron. and Astrophys.* **464** (2007), 429–435.
- [Jin and Levermore 1996] S. Jin and C. D. Levermore, “Numerical schemes for hyperbolic conservation laws with stiff relaxation terms”, *J. Comput. Phys.* **126**:2 (1996), 449–467. [MR 97g:65173](#) [Zbl 0860.65089](#)
- [LeVeque 1992] R. J. LeVeque, *Numerical methods for conservation laws*, 2nd ed., Lectures in Mathematics ETH Zürich, Birkhäuser Verlag, Basel, 1992. [MR 92m:65106](#) [Zbl 0723.65067](#)
- [LeVeque 2002] R. J. LeVeque, *Finite volume methods for hyperbolic problems*, Cambridge Texts in Applied Mathematics, Cambridge University Press, Cambridge, 2002. [MR 2003h:65001](#) [Zbl 1010.65040](#)
- [Levermore and Pomraning 1981] C. D. Levermore and G. C. Pomraning, “A flux-limited diffusion theory”, *Astrophys. Journal* **248** (1981), 321–334.
- [Lowrie and Morel 2001] R. B. Lowrie and J. E. Morel, “Issues with high-resolution Godunov methods for radiation hydrodynamics”, *Journal of Quant. Spect. and Radiative Transfer* **69** (2001), 475–489.
- [Lowrie et al. 1999] R. B. Lowrie, J. E. Morel, and J. A. Hittinger, “The coupling of radiation and hydrodynamics”, *Astrophys. Journal* **521** (1999), 432–450.
- [Mihalas and Klein 1982] D. Mihalas and R. Klein, “Solution of the time-dependent inertial-frame equation of radiative transfer in moving media to $O(v/c)$ ”, *J Comp Phys* **46** (1982), 97–137.
- [Mihalas and Mihalas 1984] D. Mihalas and B. W. Mihalas, *Foundations of radiation hydrodynamics*, Oxford University Press, New York, 1984. [MR 86h:85004](#) [Zbl 0651.76005](#)
- [Miniati and Colella 2007] F. Miniati and P. Colella, “A modified higher order Godunov’s scheme for stiff source conservative hydrodynamics”, *J. Comput. Phys.* **224**:2 (2007), 519–538. [MR 2008c:76068](#) [Zbl 1117.76039](#)
- [Minion 2003] M. L. Minion, “Semi-implicit spectral deferred correction methods for ordinary differential equations”, *Commun. Math. Sci.* **1**:3 (2003), 471–500. [MR 2005f:65085](#) [Zbl 1088.65556](#)

- [Pomraning 1973] G. C. Pomraning, *The Equations of Radiation Hydrodynamics*, Pergamon Press, Oxford, 1973.
- [Roe 1981] P. L. Roe, “Approximate Riemann solvers, parameter vectors, and difference schemes”, *J. Comput. Phys.* **43**:2 (1981), 357–372. [MR 82k:65055](#) [Zbl 0474.65066](#)
- [Stone et al. 1992] J. M. Stone, D. Mihalas, and M. L. Norman, “ZEUS-2D: a radiation magnetohydrodynamics code for astrophysical flows in two space dimensions, III. The radiation hydrodynamic algorithms and tests”, *Astrophys. Journal Supp.* **80** (1992), 819–845.
- [Stone et al. 2008] J. M. Stone, T. A. Gardiner, P. Teuben, J. F. Hawley, and J. B. Simon, “Athena: a new code for astrophysical MHD”, *Astrophys. Journal Supp. Ser.* **178** (2008), 137–177.
- [Trebotech et al. 2005] D. Trebotich, P. Colella, and G. H. Miller, “A stable and convergent scheme for viscoelastic flow in contraction channels”, *J. Comput. Phys.* **205**:1 (2005), 315–342. [MR 2132311](#) [Zbl 1087.76005](#)

Received February 18, 2008. Revised November 28, 2008.

MICHAEL DAVID SEKORA: sekora@math.princeton.edu

Program in Applied and Computational Mathematics, Princeton University, Princeton, NJ 08540, United States

JAMES M. STONE: jstone@astro.princeton.edu

Department of Astrophysical Sciences, Princeton University, Princeton, NJ 08540, United States